Microsyst Technol (2007) 13:1567–1573
DOI 10.1007/s00542-006-0344-3

TECHNICAL PAPER

Effect of surface finish of substrate on mechanical reliability of In-48Sn solder joints in MOEMS package

Ja-Myeong Koo · Seung-Boo Jung

Received: 24 June 2006 / Accepted: 20 November 2006 / Published online: 4 January 2007

Abstract The interfacial reactions and shear properties of the In-48Sn (wt.%) ball grid array (BGA) solder joints after bonding were investigated with four different surface finishes of the substrate over an underlying Cu pad: electroplated Ni/Au (hereafter E-NG), electroless Ni/immersion Au (hereafter ENIG), immersion Ag (hereafter I-Ag) and organic solderability preservative (hereafter OSP). During bonding, continuous $AuIn_2$, $Ni_3(Sn,In)_4$, and $Cu_6(Sn,In)_5$ intermetallic compound (IMC) layers were formed at the solder/E-NG, solder/ENIG and solder/OSP interfaces, respectively. The interfacial reactions between the solder and I-Ag substrate during bonding resulted in the formation of $Cu_6(Sn,In)_5$ and $Cu(Sn,In)_2$ IMCs with a minor Ag. The In-48Sn/I-Ag solder joint showed the best shear properties among the four solder joints after bonding, whereas the solder/ENIG solder joint exhibited the weakest mechanical integrity.

1 Introduction

The growth of fiber optic networks is driving the development of novel miniaturized and high performance optical components based on micro electro mechanical system (MEMS) technology (Wang et al. 2005). These needs for the micro optical electro mechanical systems (MOEMS) have pushed the development of area-array packages, such as ball grid array (BGA), wafer level package (WLP), and flip-chip, due to their smaller package size, more input/output (I/O) pins and higher electrical performance. For the MOEM package, the area-array package using solder materials is simpler to process than the thermosonic bonding process using gold or aluminum metal bumps, and has better electrical performance and mechanical properties than the bonding process using conductive adhesives. In the area-array package, the solder joints provide a path for the dissipation of the heat generated by the device as well as furnish the electrical and mechanical connections between the device and substrate (Koo et al. 2005). Therefore, the reliability of solder joints has been a crucial issue in the MEMS and MOEMS packaging industries.

Essential solder materials for the MOEM package can be categorized as tin-lead (Pb-Sn), gold-tin (Au-Sn), indium (In) and indium-tin (In-Sn) (Mickelson et al. 1997). The solder assembly using Sn-Pb solder has been the most popular approach. However, electrical and electronic equipment (EEE) manufacturers are showing more and more interest in the development of Pb-free solders and their soldering processes, due to the increasing environmental awareness of society, upcoming legislation on the use of Pb such as the waste of electrical and electronic equipment (WEEE) and restriction of hazardous substances (RoHS) directives and the tremendous market potential for 'green' products (Koo and Jung 2005). The Au-Sn solder shows the low-creep behavior, but induces the residual stress at the joint interface during bonding and system use due to its high stiffness and bonding temperature. Pure In solder exhibits excellent heat and

J.-M. Koo · S.-B. Jung (✉)
School of Advanced Materials Science and Engineering, Sungkyunkwan University, 300 Cheoncheon-dong, Jangan-gu, Suwon 440-746, Republic of Korea
e-mail: sbjung@skku.ac.kr

electrical conductivity, but has poor creep resistance (Mickelson et al. 1997). In this respect, eutectic In-Sn (In-48 wt.% Sn) solder alloy is considered as a Pb-free solder material with good potential in the MOEMS package, due to its very low melting point, great ductility and long fatigue life (Mickelson et al. 1997; Koo and Jung 2005; Morris et al. 1993). While industrial interest in the In-Sn solder is increasing, there has been relatively little fundamental research on their bonding characteristics and mechanical reliability (Morris et al. 1993).

During the bonding process, it is inevitable that the IMCs form and grow at the solder/substrate interface (Koo and Jung 2005). The formation of a thin IMC layer between the molten solder and substrate during bonding is essential to the bondability of these two materials, while the excessive formation of the IMC at the interface weakens the solder joints. The metallurgical and mechanical properties of the solder joints formed during bonding significantly depend on the surface finish of the substrate as well as the solder material. With the adoption of Pb-free solders in the packaging technology, the selection of an appropriate metallization on a substrate plays is coming to play an increasingly important role in the development of reliable solder joints (He et al. 2004). Because the In-48Sn (wt.%) alloy has the low solubility and dissolution rate of Au in the molten solder at a bonding temperature, the Au layer, which is a typical surface finish of the substrate in the MOEMS package, reacts with the In-48Sn solder to form a brittle $AuIn_2$ IMC layer at the interface (Koo and Jung 2005). Therefore, the application of the In-48Sn solder joint has been limited in MEMS and MOEMS systems (Mickelson et al. 1997). The organic solderability preservative (OSP) surface finish has several advantages, such as its good wetting property, low cost, and simple processing steps, while the In-Sn/Cu system exhibits fast IMC growth to consume the Cu layer rapidly (Chuang et al. 2002). The electroless Ni/immerstion Au (ENIG) surface finish may provide the key to successful application of In-48Sn solder, due to its thin Au layer, while the Ni_3P formed at the interface between $Ni_3(Sn,In)_4$ IMC and Ni-P substrate can weaken the solder joint (Ho et al. 1999). The immersion Ag (hereafter I-Ag) surface finish provides the excellent solderability and electrical property, but neither the interfacial reaction nor mechanical property of In-Sn/I-Ag solder joint has been reported yet.

In this work, the interfacial reactions and shear properties of the In-48Sn solder joints with the different surface finishes of the BGA substrate after bonding were investigated for the application of the In-48Sn solder in MOEM packages. Four commercial surface finishes were examined in this work: electroplated Ni/Au (hereafter E-NG), ENIG, I-Ag, and OSP over an underlying Cu pad.

2 Experimental procedure

2.1 Sample preparation

The solder balls used in this study were In-48Sn (wt.%) solder spheres having a diameter of 500 μm (Indium Corporation, USA). The substrate was a FR-4 BGA substrate. The solder bonding pad was designed as a solder mask defined (SMD) type with a pad opening of 460 μm in diameter, a pad pitch of 2 mm in length, and a solder mask (or side wall) of 10 μm in thickness. Four surface finishes of the substrate were examined in this study: electroplated Ni (7 μm)/Au (0.7 μm), electroless Ni-P (5 μm)/immersion Au (0.15 μm), I-Ag (0.7 μm), and OSP over an underlying Cu (30 μm) pad. The electroless plated Ni layer contained about 15 at.% P and had an amorphous structure. The BGA substrates were cleaned using an ultrasonic cleaner, and then dried with hot air. The solder balls were dipped into rosin mildly activated (RMA) flux and placed on the pads of the BGA substrates. All of the samples were bonded in a reflow machine (SAT-5100 + profile temperature raise heater, Rhesca Co., Japan). The heating rate, bonding temperature and time were 1.5°C/s, 150 ± 3°C and 100 s, respectively. After bonding, all samples were air-cooled to room temperature. The soldering process was carried out in a nitrogen atmosphere to prevent oxidation of the samples. The oxygen concentration in the bonding furnace was measured using an oxygen analyzer (MAXO2, Maxtec™, USA) and kept below 0.1% during the bonding process. The samples were cleaned using an ultrasonic cleaner with a flux remover after the bonding process.

2.2 Observation of microstructure

Upon completion of the bonding process, the specimens were mounted in cold epoxy, ground using 100, 400, 1,200, 1,500, and 2,000-grit SiC papers through a row of solder balls and polished with 0.3 μm Al_2O_3 powder. The microstructures of the samples were observed using a scanning electron microscope (SEM) in back-scattered electron imaging mode (BEI). For more accurate observation of the microstructures, solder was selectively etched with an etching solution consisting of 80 vol.% H_2O, 10 vol.% HF, and 10 vol.% H_2O_2. Elemental analysis was also carried out using an energy

dispersive X-ray spectroscopy (EDS). For each sample, the area of the IMC formed at the interface was measured using an image analyzer (Image tool, UTHCSA Co., USA). The measured area was then divided by the width of the image, in order to estimate the average thickness of the IMC layer.

2.3 Ball shear test

The ball shear tests were conducted using a bonding tester (PTR-1000, Rhesca Co., Japan) at 3,600 ± 300 s after bonding, due to the influence of room temperature aging on the solder alloys. The experimental procedure for the BGA ball shear tests followed the JEDEC standard (JESD22-B117). Before testing, the 5 kgf load cell used in this study was calibrated using a 1 kgf standard weight. The displacement rate and probe height were 200 μm/s and 50 μm, respectively. The displacement until fracture was measured when the shear force had decreased by 67% (2/3) of its maximum value. The deformation energy was obtained from measuring the area of the *F-x* (shear force–displacement) curve using the image analyzer software. The fracture surfaces of the samples were observed using a SEM.

3 Results and discussion

3.1 Microstructure

In-48Sn solders and four different surface-finished BGA substrates were bonded successfully in a nitrogen atmosphere. Figure 1 shows the SEM micrographs of the In-48Sn BGA solder joints with different surface finishes after bonding. Based on the EDS analysis results, the bulk solder exhibited a lamellar structure consisting of β (In_3Sn) and γ ($InSn_4$) phases.

After bonding, there was a continuous facetted IMC layer, having a thickness of approximate 1.3 μm, between the solder and the topmost Au layer of the E-NG substrate, as shown in Fig. 1a. The chemical composition of the IMC layer was $In_{66.4}Au_{33.6}$ (at.%), corresponding to $AuIn_2$. Generally, the Au layer of E-NG substrate dissolved into the molten Sn-based solder to form $AuSn_4$ IMC particles at a bonding temperature within 30 s (Ho et al. 1999). However, the topmost Au layer remained even after bonding at 150°C for 100 s, because of very low solubility and dissolution rate of Au in the molten In-48Sn solder at 150°C (Lee 1997).

All Au atoms of the ENIG substrate reacted with the molten solder and spalled off to the solder during bonding, due to its thin layer thickness. Therefore, neither Au nor Au-based IMC layer could be observed at the solder/substrate interface after bonding. The reaction between the molten solder and the exposed Ni layer resulted in the formation of a very thin IMC layer, having a thickness of approximate 0.21 μm, as shown Fig. 1b. The chemical composition of the IMC layer consisted of $Sn_{45.8}Ni_{37.9}In_{16.3}$ (at.%), corresponding to $Ni_3(Sn,In)_4$. There were $Ni_3(Sn,In)_4$ cubes, marked as A in Fig. 1b, on the thin $Ni_3(Sn,In)_4$ IMC layer. Generally, the diffusivity of atoms at grain

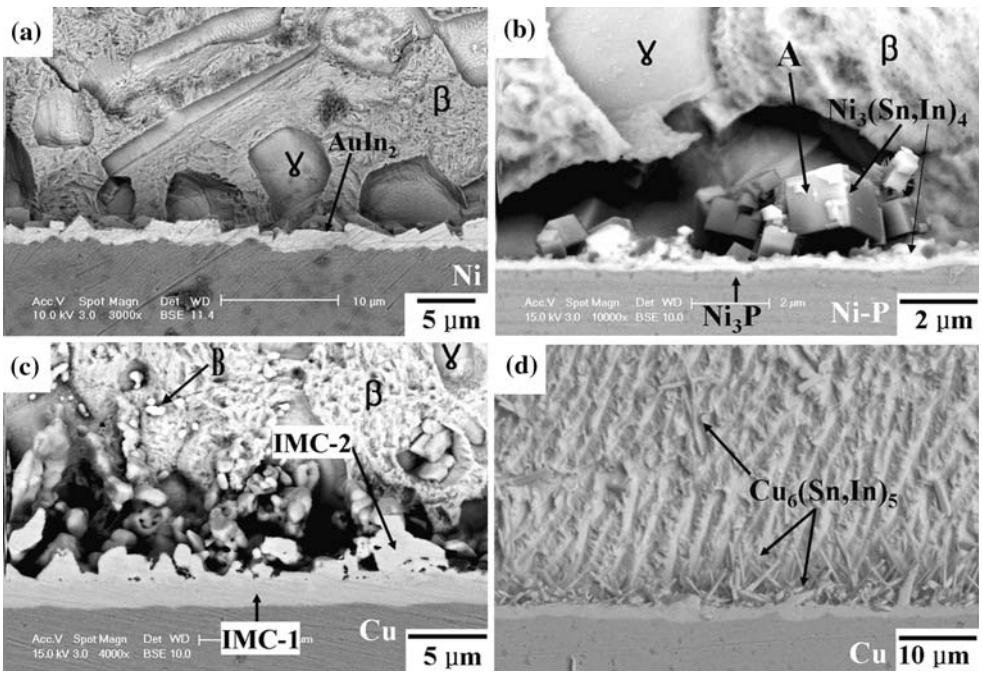

Fig. 1 Cross-sectional SEM micrographs of the interface between the In-48Sn (wt.%) solder and BGA substrate with four different surface finishes over an underlying Cu pad after reflow: **a** E-NG, **b** ENIG, **c** I-Ag, and **d** OSP

boundary is much faster than that of same atoms in the lattice (Shewmon 1989). It is suggested that the cubes were formed by the Ni atoms diffused through grain boundaries of the IMC layer rapidly and subsequently reacted with the molten solder. A very thin reaction layer could be observed at the interface between the $Ni_3(Sn,In)_4$ and Ni-P layers. The reaction layer was too thin to determine its chemical composition exactly using EDS and EPMA analyses. It was reported that the reaction layer formed between the $Ni_3(Sn,In)_4$ and Ni-P layer during liquid/solid reaction was a Ni_3P, according to the previous study using a transmission electron microscope (TEM) analysis (Koo et al. 2006).

The topmost Ag layer of the I-Ag substrate was completely depleted and disappeared at the solder/substrate interface after bonding. It is suggested that the consumption of the Ag layer was faster than that of the Au layer during bonding. There were two different IMCs at the interface between the solder and the exposed Cu layer after bonding. Based on the EDS analysis results, the chemical compositions of lower and upper IMC layers, marked as IMC-1 and IMC-2 in Fig. 1c, consisted of $Cu_{58.1}Sn_{21.0}In_{15.2}Ag_{5.6}$ (at.%), and $In_{44.1}Cu_{31.4}Sn_{16.6}Ag_{7.9}$ (at.%). As the thicknesses of the IMC-1 and IMC-2 layers were approximate 1.7 and 1.2 μm, respectively, it is suggested that the IMC-1 was the dominant phase in the In-48Sn/I-Ag interfacial reactions. These results were consistent with those in the previous studies. Kim and Jung (2005) found that the solid-state reactions between the In-48Sn and Cu substrate resulted in the formation of $Cu(In,Sn)_2$ and $Cu_6(Sn,In)_5$ IMC layers, containing $In_{52}Cu_{32}Sn_{16}$ and $Cu_{56}Sn_{24}In_{20}$, respectively. The chemical compositions of IMC-1 and IMC-2 in this work were close to those of $Cu_6(Sn,In)_5$ and $Cu(In,Sn)_2$, respectively. Therefore, it is normal that the IMC-1 and IMC-2 corresponded to $Cu_6(Sn,In)_5$ and $Cu(In,Sn)_2$, containing minor Ag, respectively. Moreover, it was observed that the intermetallics, marked as B in Fig. 1c, spalled off to the solder after bonding. The chemical compositions of these intermetallics were $Cu_{65.2}Sn_{13.3}In_{13.3}Ag_{8.2}$ and $In_{44.5}Ag_{24.7}Cu_{16.2}Sn_{14.6}$, respectively. The IMCs spalling off to the solder during bonding had more Ag content than the IMCs existed at the solder/substrate interface.

The interfacial reaction of the In-48Sn solder with the OSP substrate resulted in the formation of two different shaped IMCs, consisting of needle and planar types, as shown in Fig. 1d. However, these IMCs had a same chemical composition, $Cu_{57.4}Sn_{25.6}In_{17.0}$ (at.%), corresponding to $Cu_6(Sn,In)_5$. Sommadossi et al. (2002) reported that only a $Cu_6(Sn,In)_5$ IMC, having two different morphologies, was formed at the interface after bonding below 200°C. Laurila et al. (2005) suggested that the needle-shaped IMC was formed by the rapid dissolution of Cu in the Sn-based molten solder and then the local constitutional supercooling of the molten solder. These results were consistent with our results. The needle-shaped $Cu_6(Sn,In)_5$ intermetallics were also found in the bulk solder. It is suggested that these intermetallics spalled off to the molten solder during bonding.

3.2 Ball shear test

The ball shear tests were carried out with four different surface finishes of the substrate, to investigate the effect of the surface finish on the shear properties, such as shear force, displacement until fracture, deformation energy and fracture mode, of the In-48Sn BGA solder joints after bonding. The complex shape of the solder joint made it difficult to define the shear area and gage length. In this work, therefore, the shear force, displacement until fracture and deformation energy were used to evaluate the mechanical integrity of the solder joint, instead of the shear strength, elongation and toughness, respectively.

Figure 2 shows the relationship between the shear forces of the In-48Sn solder joint and the surface finish of the BGA substrate after bonding. The In-48Sn/E-NG and In-48Sn/ENIG solder joints showed the highest and lowest shear forces among the four different solder joints. The shear force with E-NG was 1.4 times higher than that with ENIG. The shear force of the In-48Sn/I-Ag solder joint was a little higher than that of the In-48Sn/OSP solder joint.

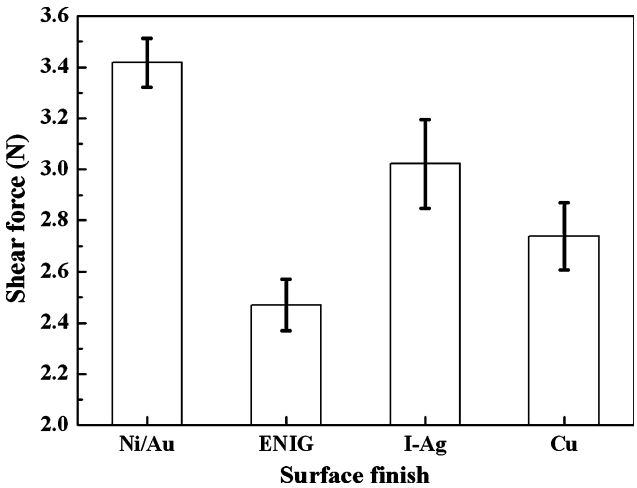

Fig. 2 Shear force of the In-48Sn (wt.%) solder joints with four different surface finishes of the BGA substrate after bonding

Figure 3 shows the relationship between the displacement until fracture of the In-48Sn solder joint and the surface finish of the BGA substrate after bonding. The values for the I-Ag and OSP surface finishes, forming the Cu-based IMCs at the interface, were higher than those for the E-NG and ENIG surface finishes. In particular, the In-48Sn/I-Ag solder joint showed the highest displacement until fracture among four different solder joints. The value with I-Ag was 1.6 times higher than that with ENIG.

Figure 4 shows the relationship between the deformation energy of the In-48Sn solder joint and the surface finish of the BGA substrate after bonding. The deformation energy strongly depended on the displacement until fracture, rather than the shear force. The In-48Sn/I-Ag and In-48Sn/ENIG solder joints exhibited the excellent and worst deformation energy among four different solder joints. The value with I-Ag was 2.1 times higher than that with ENIG.

The cracks propagated along the weakest layer or interface, which determined the mechanical integrity of the solder joint. Therefore, failure mode has been an important acceptance criterion of the ball shear test. Figure 5 shows the fracture surfaces after the shear tests for the In-48Sn solder joints in terms of the surface finish.

Figure 5a shows the fracture surface of the In-48Sn/E-NG BGA solder joint after bonding. There were many $AuIn_2$ intermetallics and dimples induced by the $AuIn_2$ IMC on the fracture surface. The fracture mode was a mixed mode, ductile solder fracture and brittle $AuIn_2$ fracture. According to the previous study, many $AuIn_2$ cubes were dispersed in the solder matrix after

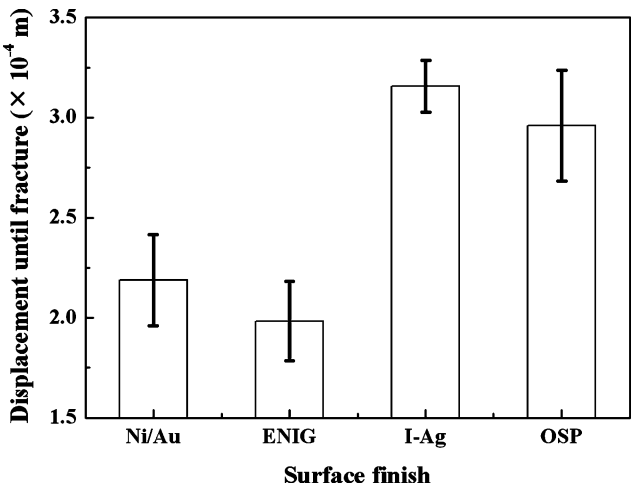

Fig. 3 Displacement until fracture of the In-48Sn (wt.%) solder joints with four different surface finishes of the BGA substrate after bonding

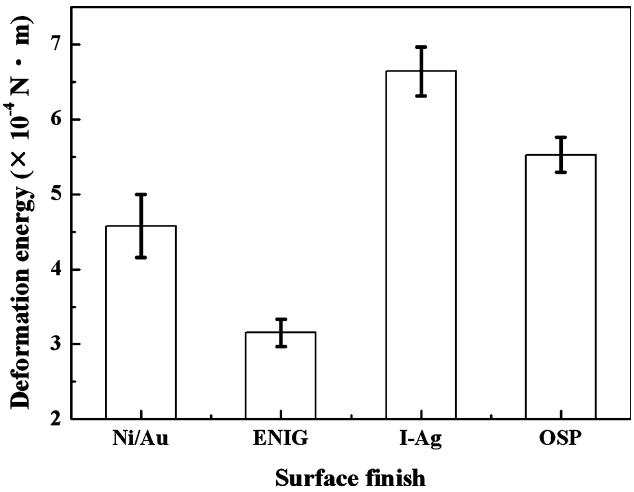

Fig. 4 Deformation energy of the In-48Sn (wt.%) solder joints with four different surface finishes of the BGA substrate after bonding

bonding of the In-48Sn and E-NG substrate (Koo and Jung 2005). Therefore, it is suggested that the high shear force was caused by the $AuIn_2$ IMC, due to the dispersion hardening, but the brittle nature and weak fracture toughness of $AuIn_2$ IMC significantly degraded the displacement until fracture and deformation energy.

The fracture surfaces of the In-48Sn/ENIG solder joints showed a mixed mode containing both ductile and brittle fractures. Many $Ni_3(Sn,In)_4$ intermetallics were observed on the fracture surface in the In-48Sn/ENIG solder joint. It is suggested that the $Ni_3(Sn,In)_4$ IMC has the weakest mechanical properties among the IMCs formed at the solder/substrate interfaces. Therefore, the formation of the continuous $Ni_3(Sn,In)_4$ IMC layer significantly degraded the mechanical integrity of the solder joint. These results showed that the ENIG surface finish was unsuitable for the In-48Sn solder.

In the In-48Sn/OSP solder joints, the cracks propagated along the bulk solder. The fracture surface showed typical ductile fracture characteristics. Therefore, the mechanical properties of the solder joints were determined by those of the bulk solder. During bonding, Cu was dissolved in the molten solder and the $Cu_6(Sn,In)_5$ IMC spalled off to the molten solder, as stated above. Therefore, the solder/OSP solder joints showed high shear properties, due to the solid-solution hardening and dispersion hardening.

The fracture characteristics of the In-48Sn/I-Ag solder joints were similar to those of the In-Sn/OSP solder joints. Moreover, the shear properties with I-Ag were higher than those with OSP. Ag in the substrate reacted with the molten solder rapidly, and many in-

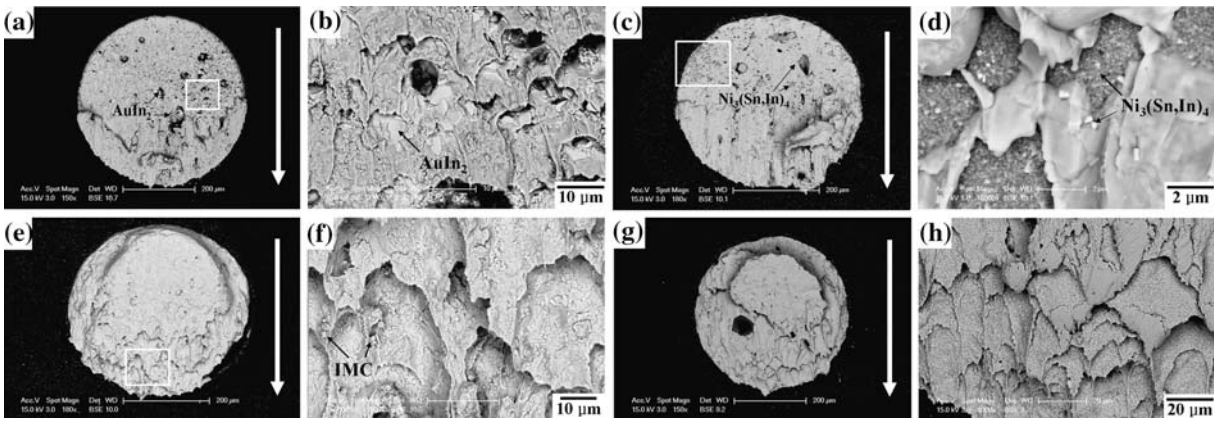

Fig. 5 SEM micrographs of fracture surfaces of the shear-tested Sn-48Sn (wt.%) BGA solder joints with four different surface finishes over an underlying Cu pad after bonding: **a** E-NG, **b** ENIG, **c** I-Ag, and **d** OSP. **b**, **d**, **f**, and **h** shows the magnified images of *rectangular regions* in **a**, **c**, **e**, and **g**

termetallics, spalling off to the solder, were observed in the bulk solder, as stated above. Therefore, it is normal that the solder joint showed the excellent mechanical properties, due to Ag-containing intermetallics dispersed in the solder matrix. The I-Ag surface finish was the most suitable metallization for improving the mechanical reliability of the In-48Sn solder among four different surface finishes.

4 Conclusions

The interfacial reactions and shear properties of the In-48Sn solder joints were investigated with the four different surface finishes of the BGA substrate after bonding, to determine the optimum surface finish of the substrate for the application of the In-48Sn solder in the MOEMS package. The results are summarized as follows.

The interfacial reaction between the solder and E-NG substrate formed a continuous facetted $AuIn_2$ IMC layer during bonding. The solder/E-NG solder joint exhibited the highest shear force, but had low displacement until fracture and deformation energy, due to the brittleness of $AuIn_2$ IMC.

During bonding, continuous $Ni_3(Sn,In)_4$ IMC and Ni_3P layers were formed at the interface between the solder and ENIG substrate. The brittleness of the $Ni_3(Sn,In)_4$ IMC layer seriously weakened the mechanical integrity of the solder joints.

$Cu_6(Sn,In)_5$ IMC, having two different morphologies, was observed after bonding. The dissolution of Cu in the molten solder and the spallation of the $Cu_6(Sn,In)_5$ IMC during bonding improved the shear properties of the solder joints.

$Cu_6(Sn,In)_5$ and $Cu(In,Sn)_2$ IMCs, containing minor Ag, were formed at the solder/I-Ag interface during bonding. The In-48Sn/I-Ag solder joint showed the best shear properties among four different solder joints after bonding, because of the IMCs dispersed in the bulk solder.

Acknowledgments This work was supported by grant No. RTI04-03-04 from the Regional Technology Innovation Program of the Ministry of Commerce, Industry and Energy (MOCIE).

References

Chuang TH, Yu CL, Chang SY, Wang SS (2002) Phase identification and growth kinetics of the intermetallic compounds formed during In-49Sn/Cu soldering reactions. J Electron Mater 31:640–645

He M, Chen Z, Qi G (2004) Solid state interfacial reaction of Sn–37Pb and Sn–3.5Ag solders with Ni-P under bump metallization. Acta Mater 52:2047–2056

Ho CE, Chen YM, Kao CR (1999) Reaction kinetics of solder-balls with pads in BGA packages during reflow soldering. J Electron Mater 28:1231–1237

Kim DG, Jung SB (2005) Interfacial reactions and growth kinetics for intermetallic compound layer between In-48Sn solder and bare Cu substrate. J Alloy Compd 386:151–156

Koo JM, Jung SB (2005) Effect of substrate metallization on mechanical properties of Sn–3.5Ag BGA solder joints with multiple reflows. Microelectronic Eng 82:569–574

Koo JM, Lee YH, Kim SK, Jeong MY, Jung SB (2005) Mechanical and electrical properties of Sn-3.5Ag Solder/Cu BGA packages during multiple reflows. Key Eng Mat 297–300:801–806

Koo JM, Yoon JW, Jung SB (2006) Interfacial reactions between In-48Sn solder and electroless nickel/immersion gold substrate during reflow process. Surf Interface Anal 38:426–428

Laurila T, Vuorinen V, Kivilahti JK (2005) Interfacial reactions between lead-free solders and common base materials. Mater Sci Eng R 49:1–60

Lee NC (1997) Getting ready for lead-free solders. Surf Mt Tech 9:65–69

Mickelson AR, Basavanhally NR, Lee YC (1997) Optoelectronic packaging. John Wiley, New York
Morris JW, Freer Goldstein JL Jr, Mei Z (1993) Microstructure and mechanical properties of Sn-In and Sn-Bi solders. JOM 45:25–27
Shewmon PG (1989) Diffusion in solids. Minerals, Metals and Materials Society, Warrendale
Sommadossi S, Gust W, Mittemeijer EJ (2002) Characterization of the reaction process in diffusion-soldered Cu/In-48 at.% Sn/Cu joints. Mater Chem Phys 77:924–929
Wang ZF, Cao W, Lu Z (2005) MOEMS: packaging and testing. Microsyst Technol 12:52–58